Journal of Catalysis **212,** 76–85 (2002)
doi:10.1006/jcat.2002.3781

Beneficial Effect of Carbon on Hydrotreating Catalysts

Cécile Glasson,* Christophe Geantet,*,[1] Michel Lacroix,* Franck Labruyere,† and Pierre Dufresne†

*Institut de Recherches sur la Catalyse, UPR CNRS 5401, 2 Av. A. Einstein, 69626 Villeurbanne Cedex, France; and †Eurecat SA, Quai Jean Jaurès, BP45, 07800 La Voulte sur Rhône, France

Received April 29, 2002; revised July 29, 2002; accepted July 31, 2002

The role of carbonaceous species on the activity of hydrotreating catalysts has been controversial for a long time. On one hand, carbon deposit is known to be one cause of catalyst deactivation, and on the other, the presence of organic thiocompounds (DMDS, tertiononyl-pentasulfide, etc.) or gas–oil during the sulfidation is recognized to provide an activity enhancement. In this work, we attempted to investigate the effect of carbon on the HDS properties of an industrial CoMo catalyst. For this purpose two carbon-containing catalysts were compared to a carbon-free catalyst. Carbon introduction was performed either by impregnating the oxide precursor with a C20 gas oil cut and subsequent drying, or by contacting the precursor with a solution of a commercial coleseed oil and further coking. After activation by H_2/H_2S, the catalytic properties of the catalysts were evaluated in thiophene conversion and real feedstock desulfurization. In both cases, and for the two preparations, a positive effect of C was observed. Several characterizations were performed (TEM, XPS, TPO, BET-BJH, EXAFS) in order to determine the role of carbon, starting from several assumptions. From these results, it was concluded that at least one identifiable beneficial effect of carbon is a geometrical one. However, structural effects may not be excluded.

Key Words: **hydrotreatment; sulfide catalysts; carbon; hydrodesulfurization.**

INTRODUCTION

It has long been recognized in practice that the activation of a hydrotreating catalyst in the presence of crude oil is more efficient than the gas-phase activation procedure. In addition, a strong dependency of the hydrodesulfurization activity (HDS) on the nature of the sulfiding agent (RSH, CH_3–S–S–CH_3, CS_2) has been observed. Later, an activity enhancement in HDS and HDN conversions of a vacuum gas–oil by using CS_2 instead of H_2/H_2S was reported by Hallie (1). On a laboratory scale, Prada Silvy *et al.* (2, 3) investigated the effect of various sulfiding agents on model reactions (thiophene HDS and cyclohexene hydrogenation) and found that butanethiol was the most efficient one. An increment in catalytic activity was recorded on using tertiononyl-pentasulfide impregnated on the precursor before sulfidation (4). This effect was related to the presence of residual carbon species and a slight enhanced dispersion of MoS_2 particles (5–11). It was also observed that in the course of the synthesis of bulk MoS_2 catalysts, the use of hydrocarbons as solvent or surfactant modifies the texture, providing higher specific surface areas and lower stacking for MoS_2 particles, as well as better stability during catalytic tests (10, 11).

Carbonaceous species have been also directly introduced in the active phase. Seiver and Chianelli patented Mo- and W-supported catalysts prepared by decomposition of $B_x[MO_yS_{4-y}]$ salts (with $M =$ Mo (or W) and $B =$ alkyldiamonium-type cation) in the presence of a thiocompound (12). The resulting phase composition $MS_{2-z}C_z$ was claimed to be more active, more selective, and more stable in HDS and HDN processes.

In fact several assumptions as to the role of C-containing molecules during the sulfidation process, have been made.

(i) A thermal effect, vaporization of gas–oil, may act as a thermal dwell which may moderate the exothermal sulfidation process, providing better control of the MoS_2 crystallite growth.

(ii) There is a geometrical effect by which a carbonaceous deposit may isolate the active sulfide crystallites and stabilize them toward sintering.

(iii) There is a support effect. Carbon species may be intercalated between the carrier and the sulfide active phase, resulting in a reduced interaction of the active phase with the support and, in turn, in enhanced activity. Carbon-covered alumina catalysts have already been reported to enhance hydrotreating properties (13).

(iv) A chemical effect, i.e., a more active carbidelike structure, "CoMoC," may be formed at the surface of the sulfide particles (14).

Recently Berhault *et al.* (15) investigated bulk MoS_2 and proposed that such carbidelike species were formed at the surface of MoS_2 particles.

As stated by Chianelli *et al.* (16), understanding the role of carbon is certainly one of the main challenges for the future of hydrotreating research.

[1] To whom correspondence should be addressed. Fax: +33 (0)4 72 44 53 90. E-mail: geantet@catalyse.univ-lyon1.fr.

0021-9517/02 $35.00

In order to get deeper insight into the role of carbonaceous species on catalytic activity, an industrial CoMo catalyst was modified with a carbon-containing agent according to two different procedures. The first method consists of an impregnation of the supported oxide precursor with a diesel oil cut and subsequent drying. In the second, the oxide precursor was contacted with a coleseed oil and coked. These precursors were further sulfided using a H_2/H_2S mixture in order to prevent additional carbon deposit. Their catalytic activities in model reactions and real feedstock conversions have been compared with that of untreated catalysts. Several characterizations were performed in order to explain the observed catalytic enhancement and to probe the various assumptions as to carbon's effect.

EXPERIMENTAL

Preparation of the Catalysts

The catalyst studied in this work is an industrial CoMo/γAl_2O_3 catalyst containing 12.3 wt% Mo and 3.0 wt% Co and having a BET area of 220 m^2/g. The introduction of carbonaceous species was performed using two different procedures. The first one (so-called gas–oil treated) consists of impregnation of the industrial catalyst with a C20 gas–oil cut using the pore filling method (Straight Run Gas Oil, $d = 0.85$ g/cm^3, 1.44 wt% S, 110 ppm N, 15% aromatics). In the second method (so-called precoked catalyst), a 10 wt% toluene solution of a commercial coleseed oil (purchased from Schmidt–Söhne, $d = 0.92$ g/cm^3) was used. After impregnation, the resulting solid was treated in a nitrogen atmosphere at 673 K for 4 h. The modified oxidic CoMo/γAl_2O_3 precursor by either method was loaded into an open-flow microreactor and sulfided at atmospheric pressure using a mixture containing 15% H_2S diluted in hydrogen (total flow, 67 cm$^3 \cdot$ min^{-1}). The temperature was then increased to the desired value at a heating rate of 5 K $\cdot$ min^{-1}. The catalyst was maintained at this temperature for 2 h. After this sulfidation step, the solid was flushed with nitrogen and quickly cooled to room temperature. The activated solids were then transferred into sealed bottles without air exposure for further physicochemical characterizations. The resulting sulfided catalysts are designated untreated, gas–oil treated, and precoked catalysts.

Catalyst Testing

The catalytic properties were determined in the HDS of thiophene and of a straight run gazoil. The thiophene HDS was carried out in an open microreactor at atmospheric pressure. The specific activities were examined at 573 K using a 2.5 mol% thiophene feed in hydrogen. Conversions were kept in the range 10–15% in order to avoid mass transfer limitations. Under these conditions, the H_2S concentration produced by the reaction never exceeds 2000 ppm. The rate of the reaction was determined at the steady state after 15 h on stream and expressed as

$$r = \frac{F_0}{m} \cdot x \quad (\text{mol} \cdot \text{s}^{-1} \cdot \text{g}^{-1}), \qquad [1]$$

where x is conversion, m is the mass of the catalyst (g), and F_0 is the molar flow of the reactant (mol/s).

Gas–oil HDS experiments were performed at 613 K and 30×10^5 Pa total pressure in a trickle-bed microreactor described in (17, 18). The main feature of this equipment is its high miniaturization, allowing catalyst testing using only a few milligrams, so steady states are reached in several hours rather than a few days, as in larger units. The gas–oil feedstock used in this work was a straight run cut with a boiling point range of 502–656 K, a density of 0.8135 g $\cdot$ cm^{-3}, and an initial sulfur content of 1.32 wt%. The 2-cm^3 reactor was loaded with about 1 g of catalyst precursor. Sulfidation was performed *in situ* with a H_2–H_2S (5%) gas mixture at 10 cm$^3 \cdot$ min^{-1} over the course of 11 h at 653 K. After sulfidation, the reactor was cooled to 373 K pressurized, the gas–oil was introduced, and the desired reaction temperature was reached. The experiments were conducted using a LHSV fixed to 8 h^{-1}.

The rate constant k_{app} was determined according to the following expression:

$$\frac{dS}{dt} = -k_{app} S^{\alpha} \qquad [2]$$

For $\alpha \neq 1$, integration of [2] gives

$$\frac{1}{(\alpha - 1)} \left[\frac{1}{S^{(\alpha-1)}} - \frac{1}{S_o^{(\alpha-1)}} \right] = \frac{k_{app}}{\text{LHSV}}, \qquad [3]$$

where S is the sulfur concentration in the effluent expressed in millimoles per gram and S_o is the initial sulfur concentration in the inlet feed (mmol $\cdot$ g^{-1}), with α being the reaction order with respect to sulfur.

LHSV is defined as

$$\frac{F_{\text{liquid}}(\text{dm}^3 \cdot \text{h}^{-1})}{V_{\text{catalyst}}(\text{dm}^3)},$$

where F_{liquid} is the inlet gas–oil flow and V_{catalyst} is the volume of catalyst loaded into the reactor.

Taking into account the small amount of catalyst required to properly run an experiment, we preferred to calculate the rate constant on the basis of a catalyst weight normalization instead of using volumes; i.e.,

$$WWH = \frac{W_{\text{liquid}}(\text{g} \cdot \text{h}^{-1})}{m_{\text{catalyst}}(\text{g})}, \qquad [4]$$

where W_{liquid} is the gas–oil weight flow and m_{catalyst} the catalyst weight.

Combining [3] and [4], the rate constant can be written as

$$k_{app} = WWH \cdot \frac{d_{oxide}}{d_{gasoil}} \cdot \frac{1}{\left(1-\frac{\%C}{100}\right)} \cdot \frac{1}{(\alpha-1)} \cdot \left[\frac{1}{S_{(\alpha-1)}} - \frac{1}{S_o^{(\alpha-1)}}\right], \quad [5]$$

where d_{oxide} is the density of the oxidic $CoMo/Al_2O_3$ catalyst ($d_{oxide} = 0.8135\ g \cdot cm^{-3}$), $WWH = 10.22\ h^{-1}$, $d_{gasoil} = 0.8497\ g \cdot cm^{-3}$, $S_o = 1.32\%$ ($0.413\ mmol \cdot g^{-1}$), %C is the weight percent of C lost during the sulfiding step, and $\alpha = 2.17$ reaction order with respect to sulfur (17). Accordingly, the rate constant was calculated according to Eq. [4] and expressed in $g^{1.17} \cdot mmol^{-1.17} \cdot h^{-1}$.

Sulfur concentration in the liquid effluents was determined by X-ray fluorescence (Horiba SLFA-1800H apparatus).

Catalyst Characterization

The textural properties of the catalysts sulfided at 673 K were determined by adsorption–desorption of nitrogen at 77 K, after evacuation for 2 h at 673K. Carbon and sulfur analyses were performed with a CS-mat 5500 analyzer (Ströhlein Instrument). XPS measurements were carried out with an ESCALAB 200R FISONS using the Al $K\alpha$ at a 1486.6-eV X-ray source. Binding energies are given by reference to Al_{2p} at 74.1 eV as internal standard. Dispersions (D), defined as the ratio of the Mo/Al or Co/Al photopeaks, were calculated after subtracting the nonlinear Shirley background and the contribution of the S_{2s} signal to the Mo 3d signals.

High-resolution electron microscopy examinations were performed with a Jeol 2010 (200 kV) instrument fitted with a UHP polar piece (resolving power, 0.19 nm). After being sulfided, the solid was immediately immersed into ethanol at room temperature and ultrasonically dispersed. The suspension was collected on a carbon-coated copper grid (200 mesh). Particle size distribution was determined by counting particles on several pictures at randomly different zones containing a few tens of particles. Ideally, representative distribution is established by counting about 1000 particles; in our case counting was performed on more than 800 particles (see Table 4.). The average particle size ($\bar{L}$) as well as the mean stacking ($\bar{N}$) was calculated according to the first moment of the distribution:

$$\bar{L} \text{ or } \bar{N} = \frac{\sum_{i=1}^{n} n_i L(\text{or } N)i}{\sum_{i=1}^{n} n_i}. \quad [6]$$

Temperature-programmed oxidation (TPO) experiments were conducted in order to test the reactivity of the C species remaining on both catalysts after sulfidation. These experiments were done in an open microreactor connected to a mass spectrometer equipped with a quadrupole analyzer (VG analyzer) operating in the Faraday mode. The gas was continuously sampled using a silica capillary tube heated at 353 K.

In a typical TPO run, 0.1 g of catalyst was loaded into the reactor. The reactor was purged with an Ar flow ($30\ cm^3 \cdot min^{-1}$) at room temperature and then the catalysts were dried by heating the system at 383 K in order to remove physisorbed water. The Ar flow was replaced by a flow of $50\ cm^3 \cdot min^{-1}$ of 4.45 mol% O_2 diluted in Ar and the reactor temperature was progressively increased to 1093 K. The CO_2 and SO_2 production was analyzed by recording the m/z signal intensity at 44 and 64, respectively, at 30-s intervals.

The XAFS measurements were performed in the transmission mode, in a dedicated *in situ* furnace (19), using the spectrometer installed by the French Collaborative Research Group on the BM32 beam line at the ESRF. The storage ring operated at 6 GeV in the multibunch mode (two-third filling) with a 200-mA current. Samples were pressed as pellets (diameter of 1.8 cm, $2000\ kg \cdot cm^{-2}$, thickness below 1 mm, in order to get an edge jump close to 1.5) and mounted in the sulfidation cell. The activation process was performed under H_2/H_2S (10%) flow from RT up to 673 K (rising temperature, 4 K/min; gas flow, 50 ml/min). XAFS measurements were performed after sulfidation at Co K-edge (7.709 keV; recording energy range, 7.6–9.2 keV) at room temperature. Standard analysis of the EXAFS spectra (normalization, background removal, Fourier transformation, and curve fitting) were carried out using the SEDEM software (20) with FEFF (21) theoretical phase and amplitude functions.

RESULTS AND DISCUSSION

Catalyst Composition

The chemical composition of the three catalysts is given in Table 1. The introduction of C leads to an apparent decrease of the Mo and Co loadings, since important quantities of carbon are deposited on the catalyst surface using either the gas–oil or the coleseed oil procedure. Corrected values were calculated according to

$$\text{Corrected Wt\%} = \frac{\text{Measured Wt\%}}{1 - \frac{\text{CWt\%}}{100}}, \quad [7]$$

where CWt% corresponds to the amount of C analyzed on the oxide samples. This correction allows the amount of Mo and Co present on the initial carbon-free catalyst to be recovered. According to these data, the surface carbon content is higher for the gas–oil-impregnated solid than for the coked catalyst precursor. This result could be easily interpreted because after gas–oil impregnation, the resulting wet material was only slightly dried so that the majority of the hydrocarbon cut remained adsorbed on the catalyst surface.

TABLE 1

Composition of Untreated, Gas–Oil-Treated, and Precoked Catalysts

Sample	Element	Wt%	Corrected wt%	Atomic loading ($at \cdot nm^{-2}$)	$r1$ Co/(Co + Mo)	$r2$ C/(Co + Mo)
Untreated	Mo	12.3	—	3.8	0.29	—
	Co	3.0	—	1.5		
Gas–oil treated	Mo	9.6	12.1	3.6		
	Co	2.6	3.3	1.6	0.31	11.7
	C	20.4	25.6	60.9		
Precoked	Mo	11.5	12.1	3.7		
	Co	3.3	3.5	1.7	0.32	2.3
	C	4.9	5.1	12.6		

Figure 1 shows the evolution of the carbon content on sulfidation. The untreated catalyst exhibits a very small amount of carbon (~0.03 wt%), which could be considered a contaminant arising probably from traces of hydrocarbon in the H_2S feed tank.

On the gas–oil-treated sample, the initial high concentration of carbonaceous species continuously diminishes down to a carbon content of around 2 wt%. This content remains stable above a sulfidation temperature of 573 K. This temperature corresponds fairly well to the boiling point of the gas–oil cut used for the impregnation. This behavior strongly suggests that the majority of the adsorbed gas–oil components are weakly bonded to the catalyst surface and progressively distillates as the temperature is increased. At 573 K only the heavier molecules either present in the gas–oil or arising from oligomerization reactions of unsaturated hydrocarbons remain on the catalyst.

For the coleseed-coked catalyst the amount of carbon remains roughly constant at a level of about 4%, irrespective of the sulfiding temperature. This coke formed during the heat treatment of the impregnated precursor at 473 K is strongly anchored to the catalyst surface and the slight decrease in the carbon content observed between RT and 573 K corresponds to the elimination of coke precursor species not yet enough condensed. For both C-containing catalysts the remaining C content is rather similar to those already reported in the literature for used CoMo or NiMo systems (22).

Sulfur Content

The sulfur content was determined by chemical analysis, XPS, and EDS for each sulfidation temperature. In the latter case, it corresponds to the average data of several analyses performed with various probe sizes according to a procedure previously described (23). The three techniques provide close data. The average of the three techniques, reported in Fig. 2, show that the atomic S/(Co + Mo) ratio

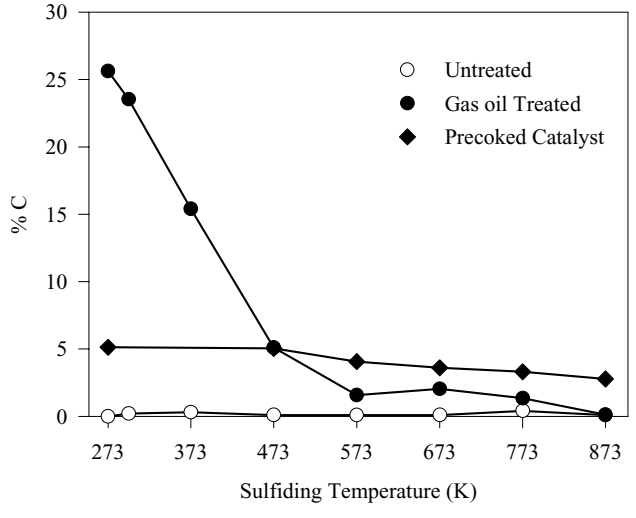

FIG. 1. Evolution of carbon content (wt%) on $CoMo/Al_2O_3$ on sulfidation.

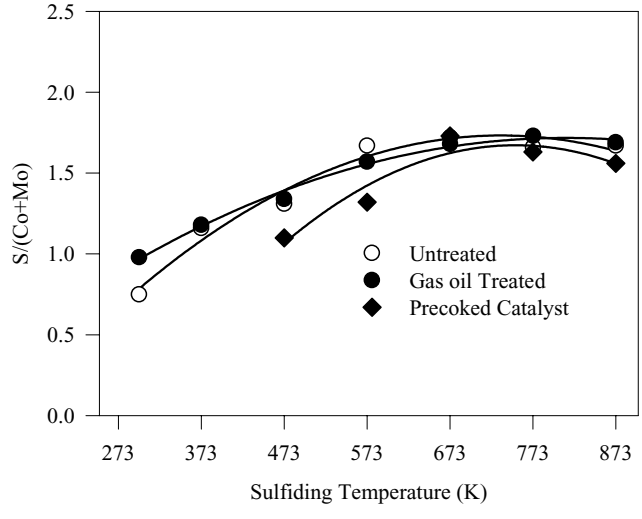

FIG. 2. Variation of the atomic S/(Co + Mo) ratio versus sulfiding temperature.

TABLE 2

Catalytic Properties of Untreated and Treated Catalysts for the Conversion of Thiophene and Gas–Oil

Sample	Thiophene conversion rate r ($\mu mol \cdot g^{-1} \cdot s^{-1}$)	Rate constant k for gas oil conversion ($g^{1.17} \cdot mmol^{-1.17} \cdot h^{-1}$)
Untreated	1.62	36
Gas–oil treated	2.57	49
Precoked	2.45	52

increases with the sulfiding temperature and levels off at 673 K. From these data it appears clearly that the presence of gas–oil does not affect the overall sulfidation of the CoMo system, since both curves superimpose. By contrast, the presence of coke delays the transformation of the Co and Mo oxides into the corresponding sulfides. At 673 K all catalysts have almost the same sulfur composition and the observed S/(Co + Mo) atomic ratio corresponds to the theoretical one assuming that Co and Mo are completely sulfided.

Catalytic Activity

It is known that the HDS activity strongly depends on the sulfidation state of the Co and Mo cations, which affects the relative proportion of the active CoMoS phase. For this reason the activity of the catalysts was determined after an *in situ* sulfidation at 673 K. The thiophene HDS activity of the three samples is reported in Table 2. The results show about a 60% increase in the overall catalytic activity due to the presence of carbon. Detailed analysis of the gas-phase composition did not evidence any modification of the selectivity toward the formation of butenes and butane. Similarly, the apparent activation energy is almost the same for the three catalysts (80 kJ/mol $< E_a <$ 84 kJ/mol). This indicates that the presence of carbon presumably modifies the number of active sites rather than their nature. In order to confirm this hypothesis the activity of the catalyst was determined in more realistic experimental conditions using directly a gas–oil as inlet reactant feed. The variations in the rate constant calculated from Eq. [5] as a function of the time on stream are reported in Fig. 3. The carbon-free catalyst exhibits a noticeable deactivation; i.e., the activity measured after 18 h on stream is about 25% lower than the initial one. By contrast, the gas–oil-pretreated solid shows a remarkable stability on time on stream while the initially more active coked catalyst slightly deactivates. The catalytic activities of the three catalysts determined after 18 h time on stream are given in Table 2. As for thiophene HDS model reaction, the presence of C during the activation of the catalyst precursors resulted in a positive effect in the HDS of a real gas–oil-cut feedstock.

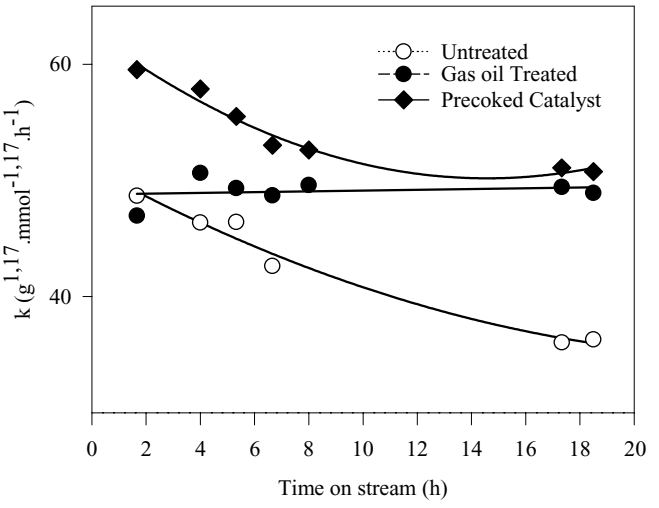

FIG. 3. Reaction rate constant of crude oil conversion as a function of the catalyst time on stream.

Solid Characterizations

Adsorption isotherms of nitrogen were first carried out to check whether the presence of carbon affects the porosity of the catalysts. These experiments were performed on the systems sulfided at 673 K. The data are presented in Fig. 4. According to the usual classification, type IV isotherms are observed for the three samples. The average pore size of pore volume distribution calculated from the BJH equation conjointly with the measured BET area and the pore volume are reported in Table 3. As shown from the isotherms, the introduction of carbon does not significantly modify the solid porosity. Carbon induces only a small decrease in the overall pore volume and/or of the mean pore size. It should be pointed out that these results differ from the data reported for used catalysts containing a similar amount of carbon (25). Used-catalyst deactivation is often ascribed to

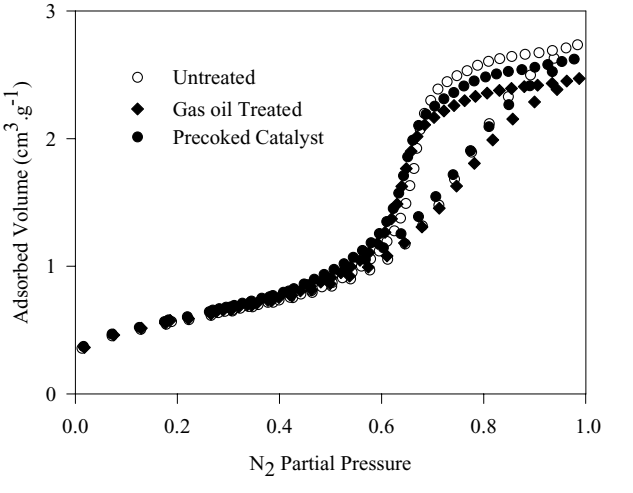

FIG. 4. Adsorption isotherms of the samples measured after sulfidation at 673 K.

TABLE 3

Textural Properties of Three Catalysts Sulfided at 673 K

Sample	BET surface area (m^2/g)	Pore volume (cm^3/g)	Average pore size (nm)
Untreated	200	0.42	3.0
Gas–oil treated	211	0.40	2.8
Precoked	204	0.38	2.7

a partial blocking of the pore entrance, leading to a decrease in accessibility of the reactants to the active sites (24, 25).

Reactivity of C Deposits

The evolution of the SO_2 and CO_2 signals produced during a TPO experiment is shown in Figs. 5A and B, respectively. The SO_2 profile exhibits two mains peaks, whose maxima are detected at around 535 and 650 K. The position of the low-temperature peak agrees very well with earlier data reported by several authors for alumina-supported CoMo catalysts and corresponds to the oxidation of the sulfur species linked to the sulfided phases. In contrast, proper assignment of the high-temperature peak is still unknown. Some authors claimed that this peak is present only on highly M-loaded catalysts (26), while others have ascribed this peak to the presence of sulfur-containing molecules in carbonaceous deposits (27, 28). From our data the latter hypothesis appears unlikely because the untreated catalyst presents this high-temperature SO_2 production and it does not contain a significant amount of C, as evidenced by the CO_2 profile presented in Fig. 5B and in agreement with the chemical analysis (see Fig. 1). Therefore it can be concluded that both SO_2 peaks could be related to the combustion of S atoms belonging to the sulfided Mo and Co phases.

TPO of the carbon-containing catalysts gives rise to only one peak of CO_2, centered at about 673 K. This temperature is in fair agreement with earlier reports concerned with used sulfide and metal catalysts, suggesting a similar nature of the C deposits. The comparison of the SO_2 and CO_2 profiles show that the CO_2 production occurred at higher temperature than that of SO_2. In fact, if we suppose the presence of a mixed CoMo sulfocarbide phase, only one part of C atoms will belong to this phase. According to the dispersion determined by TEM and the assumption that the atoms located at the edges of the particles present such a phase, we can roughly estimate the quantity of carbon atoms belonging to the so-called "CoMoC" phase, i.e., 0.4–0.6 wt% C. One can expect a measurable signal of CO_2 simultaneously appearing with the oxidation of surface S atoms (around 500 K). The absence of this peak may suggest that S and C atoms are not present on the active phase.

XPS Analysis

The Co $2p_{3/2}$ and the Mo3d photopeaks of the sulfided three catalysts at 673 K are reported in Fig. 6. Binding energies of Co $2p_{3/2}$ were found at 779.4 ± 0.2 eV for all three catalysts investigated, indicating a similar sulfidation state of the promoter. Similarly, the position as well as the XPS linewidth of the Mo 3d doublet are the same for all three catalysts. Precise decomposition of these Mo 3d signals using the nonlinear least-squares curve-fitting method based on the Marquardt–Levenberg algorithm indicates that 80% of the Mo atoms are in a formal +IV oxidation state and 20% of the overall Mo remains in a +V oxidation state. According to these experimental data it could be concluded that the presence of C does not deeply modify the nature of the alumina-supported Co and Mo cations.

The only difference observed between the three samples concerns the Co/Al and the Mo/Al ratio, which somehow reflects the overall dispersion of the sulfided phases. As reported in Fig. 7, the dispersion of the C-containing catalyst is significantly higher than that of the C-free catalyst, the C effect being more pronounced for the precoked system.

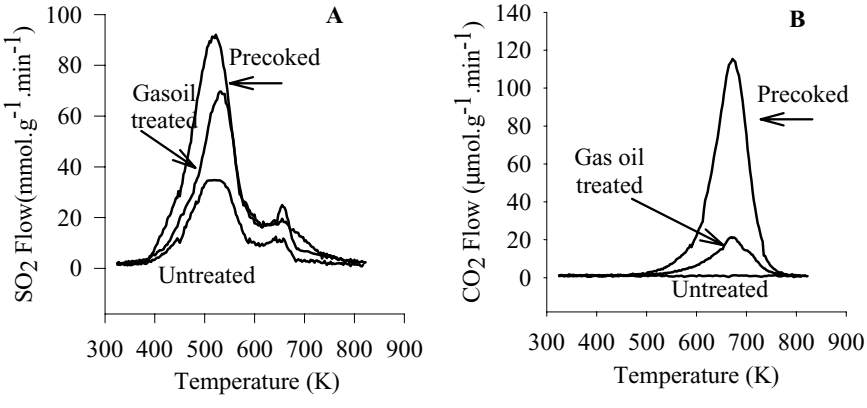

FIG. 5. Evolution of the SO_2 (A) and CO_2 (B) signals during a TPO experiment.

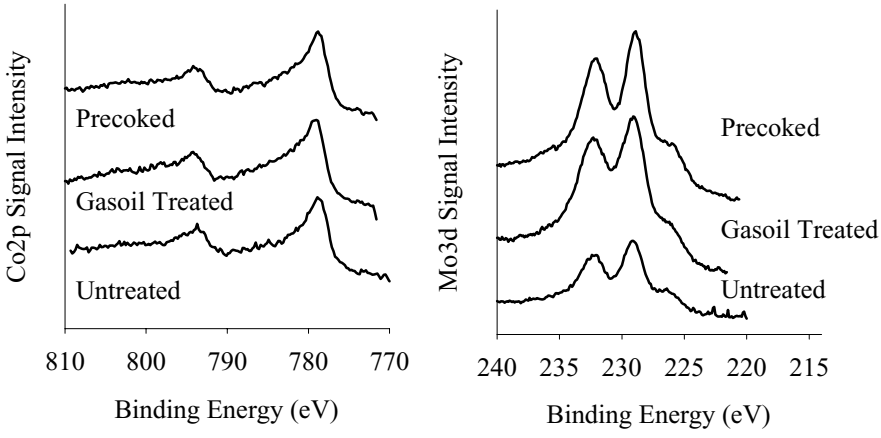

FIG. 6. Co $2p_{3/2}$ and the Mo 3d photopeaks of the sulfided catalysts.

Transmission Electron Microscopy

TEM pictures of the sulfided catalysts revealed the presence of structures typical of the layered MoS_2 phase (Fig. 8) and segregated Co_9S_8 particles were not observed. The lattice fringes have a spacing of about 0.6 nm compared to a 0.615-nm spacing for the (002) basal planes of MoS_2. Determination of the dispersion of supported sulfide catalysts remains a crucial problem, since the usual techniques, such as XRD or chemisorption, cannot be used. The controversy concerning the particle size determined by EXAFS or TEM has held on and the underestimation of the particle size by EXAFS attributed to distortions and disorders at the periphery of the slabs (29, 30). An increase in overall dispersion induced by the presence of C may arise from a diminution of the average length of the particle and/or of the number of layers forming the crystal. In order to get insight into both possibilities the three samples were examined by high-resolution electron microscopy. Table 4 reports the length and stacking distribution determined for

TABLE 4

Morphological Characteristics of MoS_2 Particles Obtained from Statistical Analysis of TEM Micrographs

Sample	Number of observed particles	Average length L (nm)	Average stacking N
Untreated	825	2.6 ± 0.06	1.95 ± 0.04
Gas–oil treated	854	2.7 ± 0.06	1.70 ± 0.04
Precoked	810	2.9 ± 0.08	1.67 ± 0.04

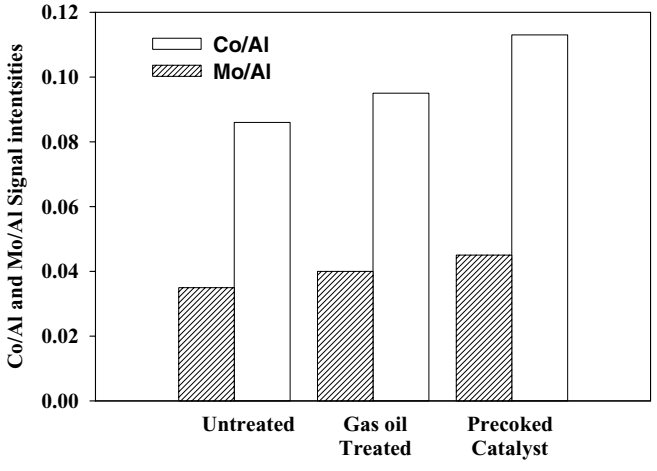

FIG. 7. Co/Al and the Mo/Al ratio determined from XPS analysis of the sulfided samples.

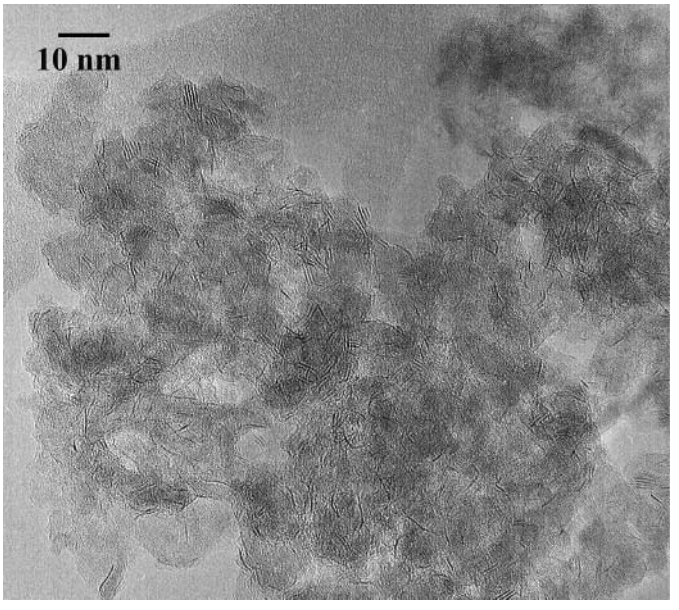

FIG. 8. TEM image of $CoMo/Al_2O_3$ reference catalysts sulfided at 673 K.

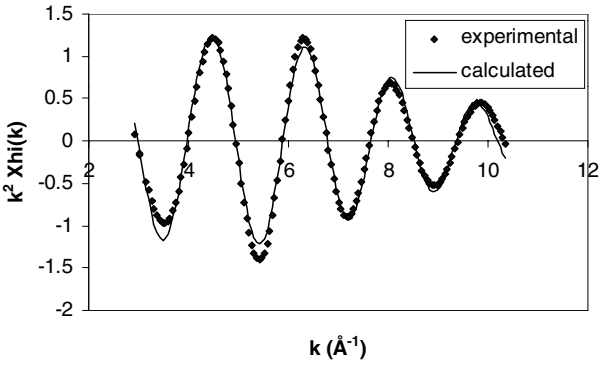

FIG. 9. Real part of inverse FFT (experimental) and best fit (calculated) obtained with one shell of sulfur neighboring atoms.

the three catalysts. Data indicate that narrow distributions of either the particle length or the number of stacked layers are obtained for these samples. According to these results, it is clear that the presence of C during the activation of the oxidic precursors leads to longer and less-stacked MoS_2 particles. Recently, a C/MoS_2 mixed layer occurring in metalloferrous black shales (31) was identified. According to the authors, this phase consists of intercalated planar aromatic species or graphitelike layers oriented parallel to MoS_2 sheets. Thus, a c-lattice parameter of 1–1.2 nm was observed. In our case, a careful examination of the interlayer spacing of the carbon-treated catalysts did not reveal such distortion of the interlayer spacing, which remains close to 0.6 nm.

TABLE 5

EXAFS Analysis at Co *K* Edge of CoMo on Alumina and Precooked CoMo on Alumina-Sulfided Catalysts

Sample	R (Å)	N	ΔE_0 (eV)	σ^2 Å^2 (10^{-3})	QF
Untreated CoMo	2.20 (4)	5.0 (2)	0.5	6.0 (5)	0.81
Precoked CoMoC	2.19 (6)	4.5 (3)	−3	6.0 (8)	0.98

Note. QF, Quality factor (20).

X-Ray Absorption

If we expect a chemical interaction of C with the active phase, Co would be more sensitive than Mo due to its location at the periphery of the particles. So we attempted to investigate the local structure of Co by EXAFS. The absorption spectra of untreated sample and precooked sample were recorded after *in situ* sulfidation at 673 K. Due to the industrial nature of the sample (various types of Co in the sample) and the RT measurements, the EXAFS data could only be used up to $k = 8$ A^{-1}. The Fourier transform (amplitude and imaginary part of the FT) presented in Fig. 9 does not evidence strong differences between the nontreated and precoked catalysts. A correct fitting of the first Co–S shell contribution is obtained (see Fig. 9) and corresponds to the parameters in Table 5. A detailed analysis of the remaining contributions, such as those performed by Bouwens *et al.* (32) on CoMo/C catalysts and evidencing Co–Mo or Mo–C

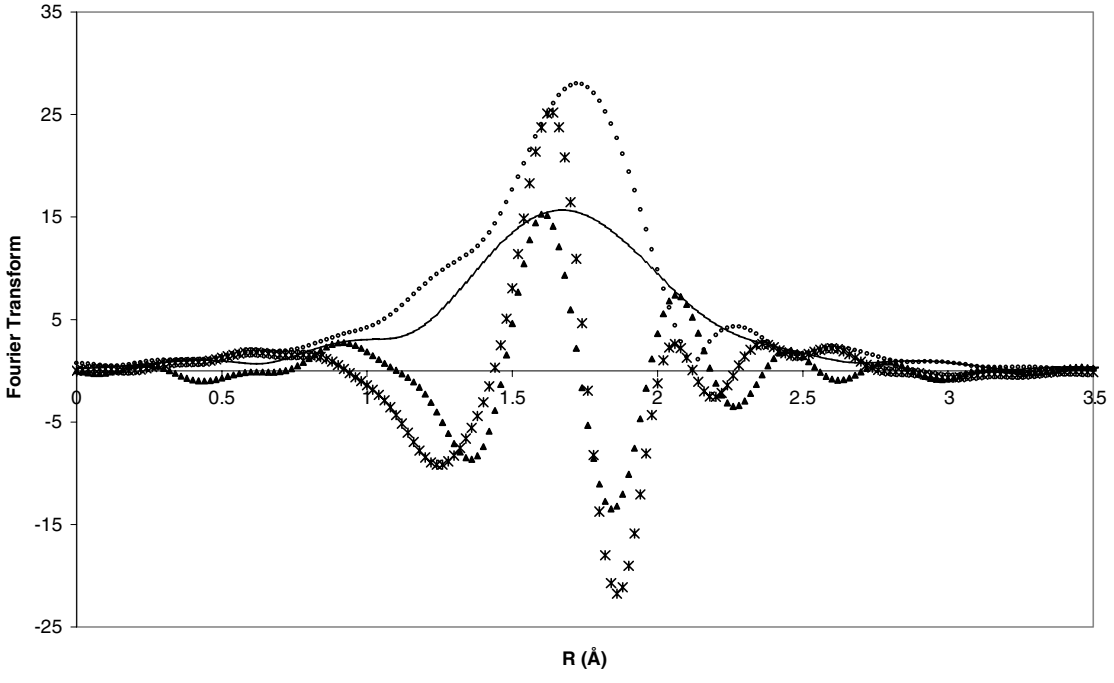

FIG. 10. Simulated Fourier transforms at Co *K*-edge with five sulfur neighbors (Amp, dotted line; Im, ∗) or one carbon and four sulfur neighbors (Amp, solid line; Im, triangles).

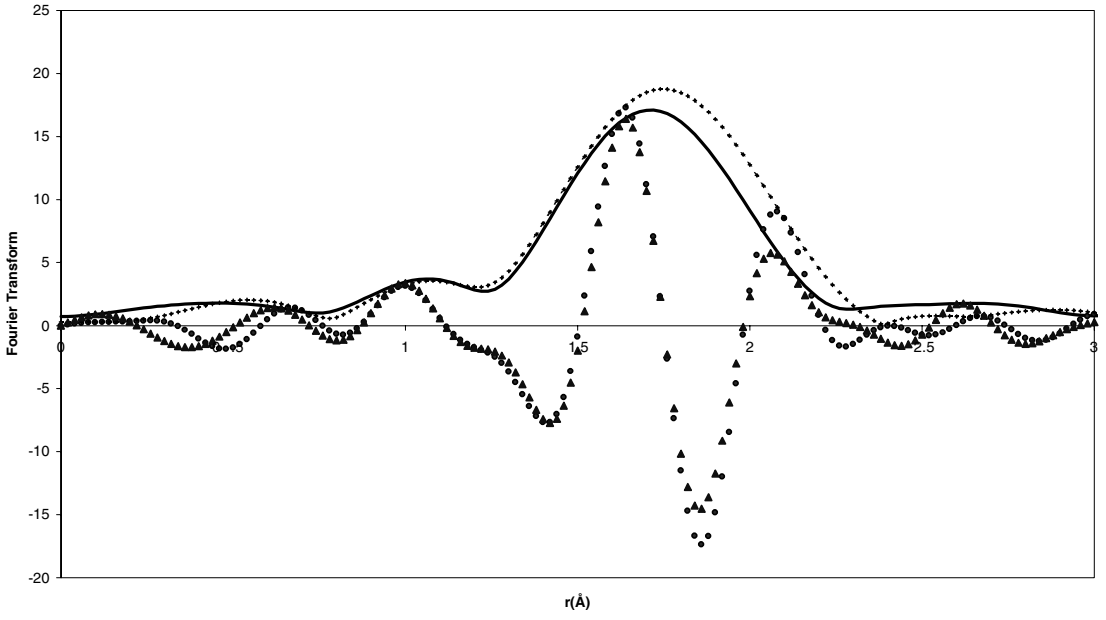

FIG. 11. Fourier transforms (k^2, $\Delta k = 2.8$–10.9 Å^{-1}), amplitude (Amp), and imaginary part (Im) at Co K-edge of CoMo (Amp, dotted line; Im, ●) and precoked catalyst (Amp, solid line; Im, triangles) after *in situ* sulfidation at 673 K.

distances, could not be achieved due to the quality of the data and the weak backscattering amplitude of C. In order to check the influence of a C neighborhood, we simulated the FT of Co surrounded by five sulfur atoms or one C atom and four sulfur atoms assuming a Co–C distance of 0.19 nm and Co–S of 0.2 nm. As shown in Fig. 10, the signature of carbon atom(s) is seen on the imaginary part of the FT in the range 1–1.5 Å (uncorrected values). If we compare it to the experimental data in Fig. 11, we cannot observe any difference between the two samples in this area, which suggests the absence of a C neighbor. This EXAFS study shows that Co atoms in the precooked catalysts are mainly surrounded by sulfur atoms and cannot reveal the presence of a carbon neighbor. Further studies using model catalysts and low-temperature measurements are required to tackle this problem.

CONCLUSION

From all these results, it is clear that reacting hydrotreating catalysts with carbon-containing reagents leads to enhanced catalytic activity (of at least 30%) and improved stability for gas–oil-treated samples. Such a positive effect is observed in the hydrotreatment of model compounds or gas–oil. We attempted to determine the effective role of carbon from the various effects mentioned in the Introduction. The use of a precoked carbon catalyst and the evolution of the extent of sulfidation show that the thermal dwell effect can be discarded. The presence of 2–4 wt% carbon on the solid does not strongly modify the overall texture of the catalyst, since only a slight plugging of the mesopores is observed. However, both the size and shape of the active particles are affected and the stacking of the slabs is also prevented. Though, we can suppose that during the activation process, migration of (Co)MoS_2 on the surface is restricted by the presence of C. This effect is reinforced by the remarkable stability of the carbon-doped catalysts, indicating that the morphology of the active phases is rapidly stabilized. Such promoting textural effect of carbon on MoS_2 has already been reported in the literature in the case of unsupported MoS_2 carbon-containing catalysts (12, 13). Chemical interaction between Mo and C has been evidenced on unsupported Mo sulfide after a batch reaction with DBT (17). However, on deactivated supported catalysts, ^{13}C NMR evidences the presence of aromatic and aliphatic carbons deposited as coke. Such compounds are supposed to represent half of the carbon present on the catalyst (33). The undetectable fraction was attributed to graphitic carbon (or surface Mo carbide species?). In such a complex system Mo–C bonds can hardly be evidenced. The comparison between the TPO patterns of the fresh and the precoked catalysts does not evidence any low-temperature CO_2 peak nor any strong difference in SO_2 production, which may suggest weakly bonded Mo–C species.

EXAFS analyses at Co K-edge shows that the majority of neighbor atoms consists of S atoms. The presence of Co–C bonds cannot be rejected; in fact Co_2C and Co_3C are metastable carbides, which decompose at nearly 673 K (34), making them much less stable than Mo_2C.

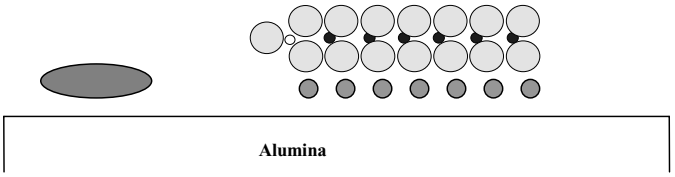

FIG. 12. Schematic representation of carboneous species (dark grey) on a CoMo on almunia sulfided catalyst (Mo, dark circles; Co, white circles; S, grey circles).

Finally, a parallel can be drawn between the effect of gazole or coleseed oil with those observed by the use of chelating agents such as NTA or EDTA (35). Several patents and academic studies were devoted to the improvement of the catalytic activity by the use of such chelating agents and various explanations were proposed. In fact this agent can also act as a carbon source which can provide some of the effects described above.

To sum up, this study evidences the positive effect of a carbon source on the activity and stability of a commercial hydrotreating CoMo catalyst. Either gas–oil or coleseed oil impregnation of a commercial catalyst provides a promoting effect on the catalytic activity in the conversion of a model molecule or a SR gas–oil. After sulfidation at 673 K, 2 to 4 wt% of C remains at the surface of the catalysts and reduces the average stacking of the MoS_2 crystallites. Thus, one identifiable effect of carbon is geometrical, but other possible effects (for example structural) cannot be excluded. A schematic representation of the role of C is given in Fig. 12. One part of carbon stood at the surface of the catalysts, similarly to the coke formed on catalytic reaction. Another part may interact during the sulfidation process and participate in the structure of the active phase as an intermediate support which stabilizes the monolayers of (Co)MoS_2 particles and prevents stacking.

ACKNOWLEDGMENTS

Y. Soldo and J. L. Hazemann and the staff of IF-CRG line are gratefully acknowledged for their assistance with XAFS measurements. We thank the French-CRG committee for providing machine time. C. Glasson thanks EURECAT SA and ADEME for a grant. ECOTECH-CNRS program is acknowledged for financial support. Y. Yoshimura is acknowledged for helpful discussions.

REFERENCES

1. Hallie, H., *Oil Gas J.* **20**, 69 (1982).
2. Prada Silvy, R., Grange, P., Delannay, F., and Delmon, B., *Appl. Catal.* **46**, 113 (1989).
3. Prada Silvy, R., Grange, P., and Delmon, B., *Stud. Surf. Sci. Catal.* **53**, 233 (1989).
4. Berrebi, G., Brevet Français 8,311,048 (1983).
5. Berrebi, G., and Roumieu, R., *Bull. Soc. Chim. Belg.* **96**, 967 (1987).
6. van Gestel, J., Leglise, J., and Duchet, J.-C., *J. Catal.* **145**, 429 (1994).
7. Dufresne, P., Brahma, N., and Girardier, F., *Rev. Inst. Français Pétr.* **50**(2), 283 (1995).
8. van Gestel, J., Leglise, J., and Duchet, J.-C., *J. Catal.* **145**, 429 (1994).
9. Dufresne, P., Brahma, N., Labruyère, F., Lacroix, M., and Breysse, M., *Catal. Today* **29**, 251 (1996).
10. Rueda, N., Bacaud, R., and Vrinat, M., *J. Catal.* **169**, 404 (1997).
11. Afanasiev, P., Xia, G. F., Berhault, G., Jouguet, B., and Lacroix, M., *Chem. Mater.* **11**, 3216 (1999).
12. Seiver, R. L., and Chianelli, R. R., US Patent 4,431,747 (1984).
13. Vissers, J. P. R., Mercx, F. P. M., Bouwens, S. M. A., de Beer, V. H. J., and Prins, R., *J. Catal.* **114**, 291 (1988).
14. Chianelli, R. R., and Berhault, G., *Catal. Today* **53**, 357 (1999).
15. Berhault, G., Mehta, A., Pavel, A. C., Yang, J., Rendon, L., Yacaman, M. J., Araiza, L. C., Moller, A. D., and Chianelli, R. R., *J. Catal.* **198**, 9 (2001).
16. Chianelli, R. R., Daage, M., and Ledoux, M. J., *Adv. Catal.* **40**, 221 (1994).
17. Letourneur, D., Bacaud, R., Vrinat, M., Schweich, D., and Pitault, I., *Ind. Eng. Chem. Res.* **37**(7), 2663 (1998).
18. Letourneur, D., Vriant, M., and Bacaud, R., *Stud. Surf. Sci. Catal.* **106**, 491 (1997).
19. Geantet, C., Soldo, Y., Glasson, C., Matsubayashi, N., Lacroix, M., Proux, O., Ulrich, O., and Hazemann, J. L., *Catal. Lett.* **73**, 95 (2001).
20. Aberdam, D., *J. Synchrotron Radiat.* **5**, 1287 (1998).
21. Rehr, J. J., Zabinsky, S. I., and Albers, R. C., *Phys. Rev. Lett.* **69**, 3397 (1992).
22. Furimsky, E., and Massoth, F., *Catal. Today* **52**, 381 (1999).
23. Glasson, C., Geantet, C., Lacroix, M., Labruyère, F., and Dusfresne, P., *Catal. Today* **45**, 341 (1998).
24. Furimsky, E., and Massoth, F. E., *Catal. Today* **17**(4), 537 (1993).
25. Absi-Halabi, M., Stanislaus, A., and Trimm, D. L., *Appl. Catal.* **72**, 193 (1991).
26. Yoshimura, Y., Matsubayashi, N., Yokokawa, H., Sato, T., Shimada, H., and Nishijima, A., *Ind. Eng. Chem. Res.* **30**, 1092 (1991).
27. van Doorn, J., Barbolina, H. A. A., and Moulijn, J. A., *Ind. Eng. Chem. Res.* **31**, 101 (1992).
28. Yoshimura, Y., and Furimsky, E., *Fuel* **65**, 1388 (1986).
29. Calais, C., Matsubayashi, N., Geantet, C., Yoshimura, Y., Shimada, H., Nishijima, A., Lacroix, M., and Breysse, M., *J. Catal.* **174**, 130 (1998).
30. Shido, T., and Prins, R., *J. Phys. Chem. B* **102**, 8426 (1998).
31. Kao, L., Peacor, D. R., Coveney, R. M., Zhao, G., Dungey, K. E., Curtis, M. D., and Penner-Hahn, J. E., *Am. Mineral.* **86**, 852 (2001).
32. Bouwens, S. M. A. M., vanVeen, J. A. R., Koningsberger, D. C., de Beer, V. J. H., and Prins, R., *J. Phys. Chem.* **95**, 123 (1991).
33. Fonseca, A., Zeuthen, P., and Nagy, J. B., *Fuel* **75**, 1363 (1996).
34. Ishida, K., and Nishizawa, T., *in* "Binary Alloy Phase Diagrams" (T. B. Massalski, Ed.), p. 835, American Society of Metals, Metal Park, Ohio (1986).
35. Thomson, M. S., European Patent 0181035B1 (1990).